

# Validation of asteroseismic fitting with the new white dwarf evolution code

Agnès Kim 

Penn State Scranton, 120 Ridgeview Drive, Scranton, PA 18447, USA  
email: [axk55@psu.edu](mailto:axk55@psu.edu)

**Abstract.** The new version of the White Dwarf Evolution Code ([Bischoff-Kim & Montgomery 2018](#)) overcomes limitations of earlier versions by utilizing MESA modules for the equations of state and opacities, now allowing regions of the model with a mix of helium, carbon, and oxygen. This single improvement allows us to almost exactly replicate models output by other stellar evolution codes. Armed with this new capability, we use as a star to fit, a hydrogen atmosphere white dwarf model from the La Plata group (using the LPCODE). We present results of fitting different subsets of periods for that model. This allows us some validation of our fitting methods, knowing exactly what properties we should be recovering in our best fit model.

**Keywords.** stars: interiors, stars: oscillations (including pulsations), stars: white dwarfs

---

## 1. Introduction

The goal of asteroseismic fitting is to produce a model that is a good representation of the star. We go from the premise that if the pulsation periods of our model match the observed pulsation spectrum, then our model matches the interior conditions and stellar parameters of the star. While we can never gain absolute knowledge of the interior structure of a star, we can check whether our tools and methods can recover the properties of a “known star”, by attempting to fit a model produced with a code other than the one used to do the fitting.

The code used to compute the models involved in the fitting process is the WDEC ([Bischoff-Kim & Montgomery 2018](#)) and the synthetic star we sought to recover was produced using the LPCODE ([Romero \*et al.\* 2012](#)). We also began to address the question of period sampling. While to our knowledge, all normal modes of vibrations should be excited in a white dwarf interior, there are damping mechanisms and observational constraints that lead to the detection of a subset of all possible modes. In some cases, we observe only a few modes (one to three), while in others we get up to a dozen mode (for DAVs and DBVs). The mix of observed frequencies also determines how well the fits are constrained. In what follows, we detail the methodology further and present some results of this exercise. We learn valuable lessons.

## 2. Method

### 2.1. Models

The fitting techniques we are testing involve the computation of model grids with WDEC and a search for the best fit model on that grid. The best fit parameters are sometimes refined via a simplex search, but we did not do that in this work. We used a DAV model from the La Plata group that had a temperature of 11,288 K, a mass of  $0.593 M_{\odot}$ , and a hydrogen layer mass of  $10^{-4.285}$ . The model was chosen to represent a typical DAV. The composition profiles of this model (the synthetic star) are shown

**Table 1.** Parameters used in the fits. For a description of each, see Bischoff-Kim (2018) and Bischoff-Kim & Montgomery (2018). For each parameter varied, we list the range followed by the step size.

Oxygen Profile	Envelope Profiles	Other
$h_1 = 0, 1; 0.1$	$M_{\text{env}} = 1.5, 10; 0.5$	$T_{\text{eff}} = 10, 000 - 13, 000; 500 \text{ K}$
$h_2 = 0, 1; 0.1$	$M_{\text{He}} = M_{\text{env}}, 10; 0.5$	$M = 0.4, 1.0; 0.05 M_{\odot}$
$h_3 = 0.68; \text{fixed}$	$x_{\text{he\_bar}} = 0.68; \text{fixed}$	$\text{MLT } \alpha = 0.65; \text{fixed}$
$w_1 = 0.44; \text{fixed}$	$\alpha_1 = 16; \text{fixed}$	
$w_2 = 0.12; \text{fixed}$	$\alpha_2 = 8; \text{fixed}$	
$w_3 = 0.41; \text{fixed}$	$M_{\text{H}} = 4.0, 10; 0.5$	
parameters of the WDEC target model		
$h_1 = 0.71$	$M_{\text{env}} = 1.6$	$T_{\text{eff}} = 11288 \text{ K}$
$h_2 = 0.77$	$M_{\text{He}} = 2.2$	$M = 0.593 M_{\odot}$
	$M_{\text{H}} = 4.24$	

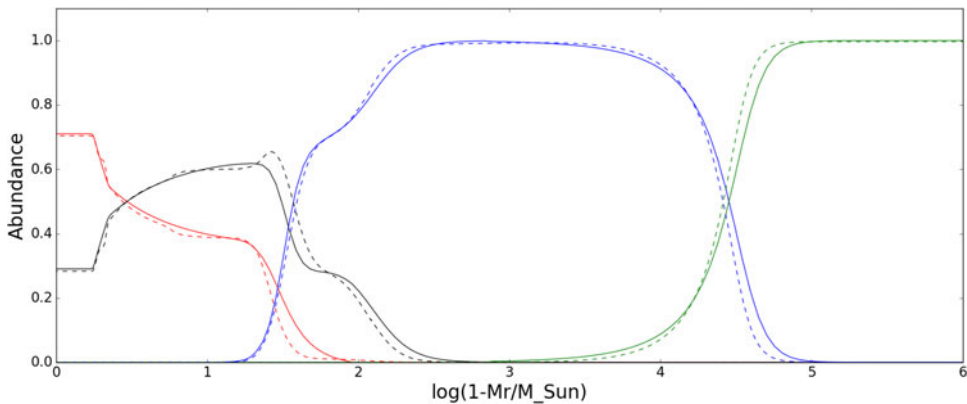


**Figure 1.** Composition profiles for the LPCODE model (dashed lines) and the matching WDEC model (solid lines). The center of the model is to the left and the surface to the right. The inner most profile (red) is oxygen, followed by carbon (black), helium (blue) and hydrogen (green).

in Fig. 1 with the dashed lines. We produced a WDEC model as close as possible to the LPCODE model. The composition profile of that model is shown with solid lines in Fig. 1. The effective temperature and mass of the model are the same as that of the LPCODE model. We call this model the “WDEC target model”. Its parameters are listed in Table 1. In the grids used here, we varied 7 parameters. We also include the values we set for the other parameters that can be varied in the fitting process. The 6 oxygen profile parameters of Table 1 define Oxygen composition profiles by providing 5 points with vertical (composition) coordinates defined by  $h_i$  and horizontal (mass coordinates) defined by  $w_i$ . The envelope profile parameters define the helium and hydrogen composition profiles by specifying the location of transition zones ( $M_{\text{env}}, M_{\text{He}}, M_{\text{H}}$ ) and how smooth the transitions are ( $\alpha_1$  and  $\alpha_2$ ).  $x_{\text{he\_bar}}$  denotes the helium abundance in the region where it is mixed with carbon.

### 2.2. Period sets and fitting

To simulate fitting a star, we must pick a set of periods to fit from the complete list of possible modes for the synthetic star. We work with three sets of periods. The first set is similar to the modes we observe in G117-B15A, where we have a consecutive sequence of three, low  $k$  modes. The second set is similar to the pulsation spectrum of EC14012, with

**Table 2.** The lists of periods (in seconds) used in our fitting exercises. For each period sampling (superstar, G117-B15A like, EC14012), we list the periods of the grid point model, the WDEC target model, and the LPCODE model, respectively (see text for more details). All periods listed are  $\ell = 1$  modes. Radial overtones ( $k$ ) are listed.

$k$	The superstar			G117-B15A like			EC14012 like		
1	129.087	140.051	135.388						
2	192.787	201.948	197.131	192.787	201.948	197.131			
3	256.689	269.803	279.542	256.689	269.803	279.541			
4	286.012	289.583	301.235	286.012	289.583	301.235			
5	304.199	315.773	325.593						
6	362.257	379.909	385.368				362.257	379.909	385.368
7	408.054	429.740	432.723						
8	462.873	484.940	491.634						
9	511.129	534.928	544.735				511.129	534.928	544.735
10	548.731	560.193	566.079				548.731	560.193	566.079
11							576.757	603.513	612.191
15							737.931	817.847	827.041
19							922.234	993.246	997.359
21							992.598	1076.844	1096.776

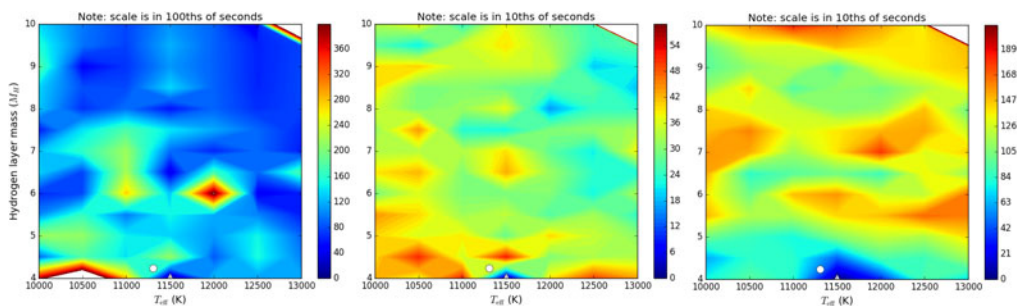


**Figure 2.** Results of the first level of fitting (fitting the periods of the model on the nearest grid point). Shown are quality of fit maps for the hydrogen layer mass. Blue indicates good fits, while red is worse. The scale shown are in the units labeled at the top of each figure and are essentially a standard deviation between the expected list of period and the periods of the models in the grid. The triangle at the very bottom of each map at  $T_{\text{eff}} = 11500$  K is the location of the best fit, while the circle is the expected location of the best fit. Left: G117-B15A like period spectrum; center: same for EC14012, right: consecutive  $k = 1 - 10$  periods.

7 higher  $k$  modes, most of them non-consecutive. The last set includes an  $\ell = 1$  sequence, complete from  $k = 1$  to 10. To our knowledge, no observed period spectrum offers such a complete sequence though some pulsating white dwarfs come close, for instance TIC 257459955 (Bell *et al.* 2019). We call this spectrum the “superstar” (2).

We performed three levels of fitting. The first one was to find the model at the grid point nearest the WDEC target model and fit the periods of that model. The best fit model in this case is a perfect fit and we expect the optimization process to find it easily. The second was to fit the WDEC target model. Lastly, we fit the periods of the LPCODE model. This last test brings us closest to the challenge of fitting an observed period spectrum. All sets of periods are listed in Table 2.

### 3. Results

In Fig. 2 we present the results of the first level of fitting (fitting the periods of the model on the nearest grid point). We focus on the fitness map for the thickness of the hydrogen layer. We show the results for all three sets of periods discussed above and

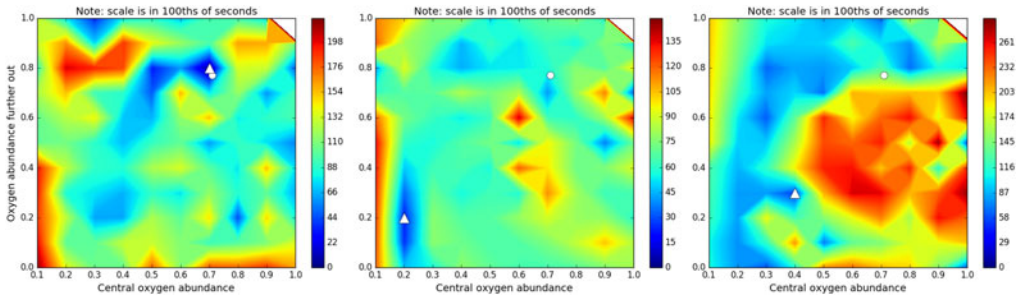


**Figure 3.** Result of the higher level fitting described in section 2.2. Shown are quality of fit maps for the core parameters for the G117-B15A like period spectrum. See caption of Figure 2 for more information. Left: fitting the grid model periods; center: fitting the target WDEC model periods, right: fitting the LPCODE model periods.

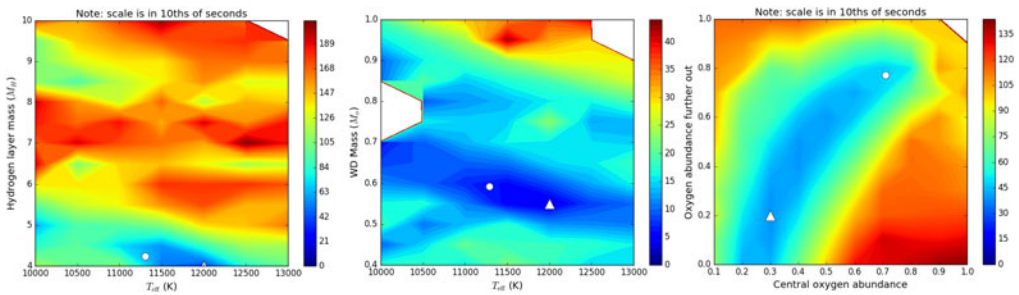


**Figure 4.** Quality of fit maps for the core parameters for the periods spectrum with the consecutive  $k = 1 - 10$   $\ell = 1$  sequence of modes. See caption of Figure 2 for more information. Left: hydrogen layer mass; center: mass and effective temperature, right: core parameters.

listed in Table 2. In rather simplistic terms, we expect the presence of higher  $k$  modes to assist in constraining the hydrogen layer mass. The transition occurs in the outer parts of the model, where higher  $k$  modes tend to be trapped. We find that indeed, we get stronger constraints with the EC14012 like spectrum and the “superstar spectrum” (where all modes from  $k = 1$  to 10 are present).

In Fig. 3, we focus on the G117-B15A like spectrum and attempt the higher level fitting described in section 2.2. We look at the fitness map for the core parameters. While we do recover the correct core parameters when fitting the grid point model (a sanity check), the method fails when we move to fitting periods of models that are off the grid, or not computed with WDEC. We do not recover the correct best fit parameters. In the case of the target WDEC model, we do find a best fit near where we expect it, but there is a much stronger minimum elsewhere in parameter space. The same is true when fitting the periods of the LPCODE model.

In Fig. 4, we examine various results of fitting the LPCODE model when using the consecutive the  $k = 1 - 10$  mode sequence. Due to the larger range of consecutive modes, we expect better results. We do get good results, with the exception again of the core parameters, even though the region of best fits does contain the correct parameters. Effective temperature is harder to constrain. It should be noted that the two core parameters have to do with the oxygen abundance in different regions of the model. We know from experience that we are more sensitive to the location of transition zones, so the results may be a little on the pessimistic side.

#### 4. Conclusion

From the numerical experiments presented here, we learn that it is a good idea to look at fitness maps to assess the presence of possible alternative best fit parameters. Constraints from spectroscopy or parallaxes can help pick the correct solution in mass and effective temperature. Fitness maps can also help determine the strength of the result of a fitting. Plots such as those in Fig. 2 can be useful in that respect. For instance, we learn that any mass and effective temperature fitting we do for G117-B15A is poorly constrained, while any fitting of the hydrogen layer mass we do for a star like EC14012 should give us a strong result. This statement comes with a caveat. Each observed period spectrum is unique and offers a different set of constraints in the asteroseismic fitting. The presence or absence of a single mode can dramatically affect the nature of the fitting (Bischoff-Kim 2017).

#### References

- Bell, K. J., Córscico, A. H., Bischoff-Kim, A., *et al.* 2019, arXiv e-prints, [arXiv:1910.04180](https://arxiv.org/abs/1910.04180)  
Bischoff-Kim, A. 2017, *European Physical Journal Web of Conferences*, 06011  
Bischoff-Kim, A. & Montgomery, M. H. 2018, *Astronomical Journal*, 155, 187  
Bischoff-Kim, A. 2018, Non-luminous sources of cooling in pulsating white dwarfs (<https://doi.org/10.5281/zenodo.1715917>).  
Romero, A. D., Córscico, A. H., Althaus, L. G., *et al.* 2012, arXiv e-prints, [arXiv:1204.6101](https://arxiv.org/abs/1204.6101)